Kirigami fabrication of shaped, flat-foldable cellular materials based on the Tachi-Miura polyhedron

Sam Calisch, Neil Gershenfeld

Abstract: *The Tachi-Miura polyhedron possesses a number of useful properties, including bidirectional, rigid flat-foldability, tailorable Poisson ratio, and tileability. This work shows how to efficiently produce shaped volumes with these properties by modifying constructions for shaped kirigami honeycombs to replace the hexagonal cells with Tachi-Miura polyhedral cells. We analyze the rigid mechanics of these Tachi-Miura honeycombs, and experimentally test the elastic behavior subject to realistic materials and boundary conditions. Finally, we prototype, fabricate, and test a running shoe sole using these techniques.*

1   Introduction

In [Miura and Tachi 10] and [Tachi and Miura 12], several rigid-foldable origami cylinders are proposed and analyzed. One example, the Tachi-Miura polyhedra, is a rigid, bidirectionally flat-foldable cylinder which is tileable. Such foldable, space-filling cylinders open the possibility of constructing cellular materials with rigid folding mechanisms. The mechanical properties of cellular materials based on the Tachi-Miura polyhedron have been analyzed in several studies, including [Yasuda et al. 13], [Yasuda and Yang 15], and [Yasuda et al. 16]. As these materials are rigidly flat-foldable, they can be used to create objects that undergo large reversible strains, with Poisson ratios determined by the Miura angle used to create the underlying polyhedra. This capability is a powerful tool for engineering compliant structures.

Physically constructing such cellular materials by simply joining many cylinders is difficult to implement at scale, but we can adapt strategies that were developed to efficiently construct origami honeycombs [Nojima and Saito 06] [Saito et al. 11] [Saito et al. 14] [Wang et al. 17]. These works show how a single sheet can be cut and folded to create a straight-walled honeycomb filling the space between two bounding surfaces. The current research extends these methods to fabricate honeycombs with Tachi-Miura polyhedra instead of hexagonal prismatic cells. These cellular materials are efficiently constructed by cutting and scoring a flat sheet which rigidly folds into the cellular material. By specifying locations of cuts, these cellular materials acquire a desired shape, just as with hexagonal honeycombs. We call such structures *Tachi-Miura honeycombs*.
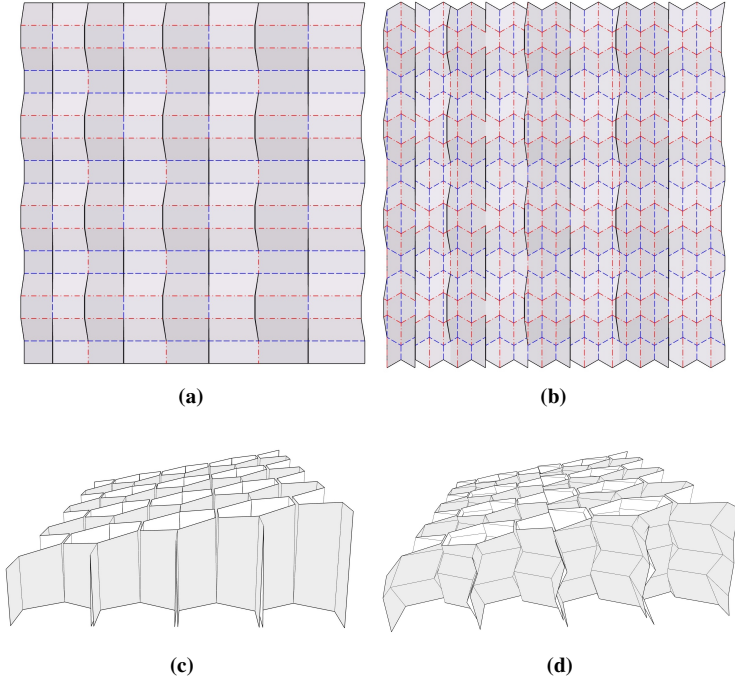
Figure 1: *A) Cutting and folding pattern for the straight-walled honeycomb (blue dashed lines denote a valley fold, red dash-dot lines denote a mountain fold, and black solid lines denote a cut), B) Cutting and folding pattern, for Tachi-Miura honeycomb, made replacing straight folds with zig-zag folds, C) Shaped straight-walled kirigami honeycomb, D) Shaped Tachi-Miura kirigami honeycomb.*

In this work, we first describe our construction for these cellular materials and characterize the rigid folding motions of the resulting cellular materials by calculating their Poisson ratios. To validate the application of these cellular materials to engineer compliant materials, we measure the mechanical response of samples under compressive loading. By varying the Miura angle of the underlying Tachi-Miura polyhedron, we can tune response to match a range of common engineering foams. We then design a prototype utilizing both the large compliance of the folding mechanism and the shape control offered by the honeycomb construction: a running shoe sole. We laser cut, fold, and test this prototype.

1.1 Pattern generation

We begin by describing our method of constructing an origami pattern for a Tachi-Miura honeycomb filling a given volume. The volume to be filled is defined as all

points $(x, y, z) \in \mathbb{R}^3$ such that $0 < x < X$, $0 < y < Y$, and

$$u(x,y) < z < t(x,y). \tag{1}$$

In other words, the volume is the space bounded by two functions u, t, restricted to a rectangular region of the $x - y$ plane. For instance, in Figure 1c, t and u are taken as linear functions describing planes.

In [Saito et al. 14, Calisch and Gershenfeld 18], methods are derived for calculating the shape and positions of the slits in Figure 1a in order to produce the honeycomb shown in Figure 1c. These methods use evaluations of the functions t and u in recursive equations to calculate these parameters. For brevity, we do not reproduce these derivations here, but refer the reader to these articles for the details of these calculations.

Our method for producing Tachi-Miura honeycombs is a direct adaptation of the method described above, motivated by modifying the cutting and folding pattern shown in Figure 1. First, we introduce some nomenclature. We distinguish *corrugation folds*, the horizontally-running folds in Figure 1a, from *strip folds*, the vertically-running folds joining adjacent cuts. Then, we conceptually subdivide the pattern into *strips*, the regions of material bounded on left and right by cuts and strip folds. For example, Figure 1a is composed of eight strips.

Within each strip, we replace each corrugation fold line with a zig-zag fold of the same mountain/valley orientation. As shown in Figure 2, these zig-zag folds make an angle of $\pm\alpha$ with the vertical axis and has a period of $2d$. Vertical mountain and valley folds are added between each vertex of the zig-zag as shown to create a Tachi-Miura quarter cylinder [Tachi and Miura 12]. We apply this modification to each strip, taking care to adjust the phase of the zig-zag fold pattern so that adjacent strips align when the strip folds are actuated.
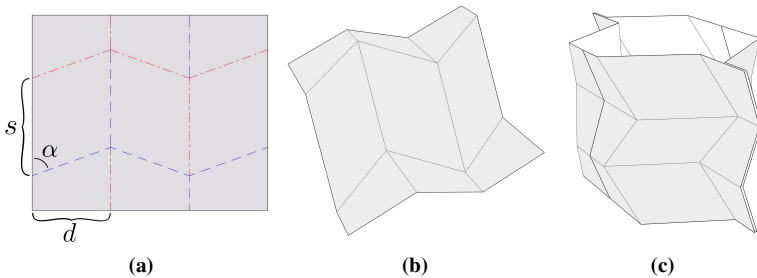

(a) **(b)** **(c)**

Figure 2: *A) Parameterized Tachi-Miura unit cell folding pattern, B) Tachi-Miura unit cell three dimensional geometry. C) The unit cell and its mirror image arranged into a Tachi-Miura polyhedron.*

This modification allows us to produce Tachi-Miura honeycombs from one sheet, but to accurately determine the shape, we must analyze the rigid folding
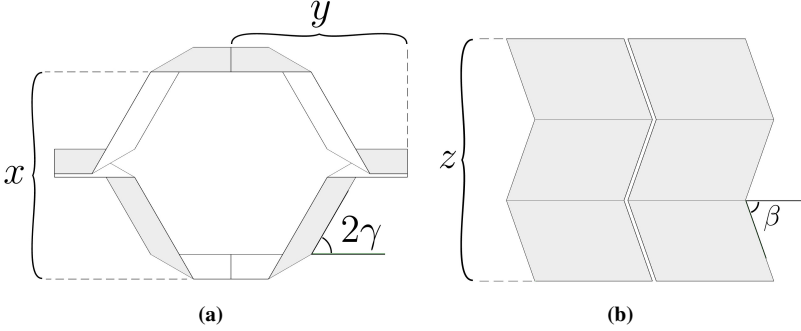
Figure 3: *A) Plan view, defining x, y, and γ, B) Altitude view, defining z and β.*

mechanism of the Tachi-Miura polyhedron. To do this, we use an angle parameterization, introduced and proven in [Miura and Tachi 10], given by the equation:

$$\tan \alpha \cos \beta = \tan \gamma \qquad (2)$$

where the *Miura angle* α sets the relationship between the exterior angle of each cell (2γ) and the dihedral angle of the trapezoidal faces (2β). These angles are shown graphically in Figure 3a.

Using these angle definitions, we define variables x, y, z for the spatial extents of a cell in each coordinate direction, shown in Figure 3b. We calculate:

$$x = 2s \sin 2\gamma \qquad y = s + s \cos 2\gamma \qquad z = Nd \sin \beta \qquad (3)$$

where N is the number of zig-zag half-periods in our strip. We see that the expressions for x and y are identical to those of a standard hexagonal honeycomb cell, while the expression for z is simply scaled by a factor of $\sin \beta$. Therefore, to accurately reproduce the shape of functions t and u, we must scale our generated patterns in the horizontal direction by a factor of $1/\sin \beta$.

We note that for functions t and u with large derivative, the intersection of the folded image of the zig-zag fold with the top or bottom surface can differ from the function's value at the base point of the zig-zag fold. This is illustrated in Figure 4, where the image of the zig-zag fold is shown in magenta. In this case, we can correct the function values used in the recursive equations by calculating the actual intersection of the zig-zag fold image with the bounding surfaces.

To do this, we define the linear segments of the magenta path by vectors $\mathbf{v}_+$ and $\mathbf{v}_-$ (shown in Figure 4b). Using the angle parameterization of the Tachi-Miura polyhedron and the parallelogram area interpretation of the cross product, we calculate

$$\mathbf{v}_+ = d \left[\cot \alpha, \cot \alpha - \frac{\cos \beta}{\sin 2\gamma}, \sin \beta \right]^\mathsf{T} \qquad (4)$$

$$\mathbf{v}_- = d \left[-\cot \alpha, -\cot \alpha + \frac{\cos \beta}{\sin 2\gamma}, \sin \beta \right]^\mathsf{T} \qquad (5)$$
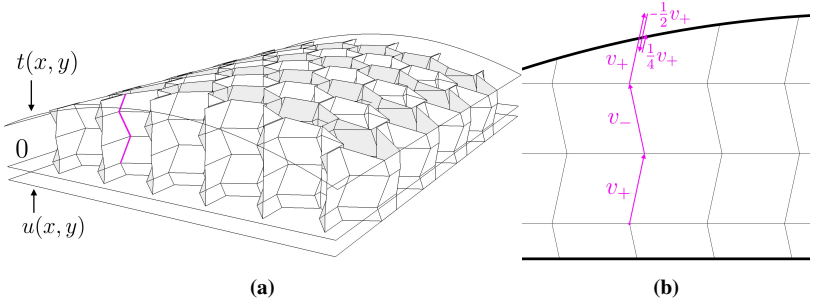
Figure 4: *A) Bounding surfaces t and u shown in reference to the z = 0 plane.
B) Calculating the intersection of the zig-zag fold image curve with the bounding
surfaces using binary search.*

Thus, to calculate the intersection point we start from a point known to lie between
t and u (shown in Figure 4 as the $z = 0$ plane). We alternatively add $\mathbf{v}_+$ and $\mathbf{v}_-$ until
we leave the valid region. At this point, we have bracketed the intersection point by
the end points of one linear segment of the zig-zag fold image path. Hence, we can
simply perform a root search (e.g. binary search) to approximate the intersection
point as accurately as is desired. For example, in Figure 4, the intersection point is
computed to be approximately $\mathbf{v}_+ + \mathbf{v}_- + \mathbf{v}_+ - \frac{1}{2}\mathbf{v}_+ + \frac{1}{4}\mathbf{v}_+$ away from the starting
point.

Finally, we also note that for functions t and u with large curvature, self-
intersections of the flat folding pattern can occur as a result of the zig-zag phase
shift. In practice, these are small, and for the purposes of the present work, we
ignore them. With these corrections and caveats, our modification of the kirigami
honeycomb pattern produces Tachi-Miura honeycombs filling the same volume.

2   Results

2.1   Poisson Ratios

To analyze the mechanical behavior of these Tachi-Miura honeycombs, we first
calculate their Poisson ratios (i.e., negative the ratio of strains between coordinate
directions during the folding motion). We start from the expressions derived above
for the x, y, and z extents, calculating the Poisson ratios in terms of α and γ. Our
expressions are similar to those derived in [Yasuda and Yang 15] but with a pa-
rameterization (shown in Figure 3) of cell extents that generalizes to volumes of
adjacent cells (instead of applying to single cells).

To derive the poisson ratios of these structures, we must write expressions for
the strains $\varepsilon_x = dx/x$, $\varepsilon_y = dy/y$, and $\varepsilon_z = dz/z$. Towards this end, we take deriva-
tives of the spatial extents relative to γ:

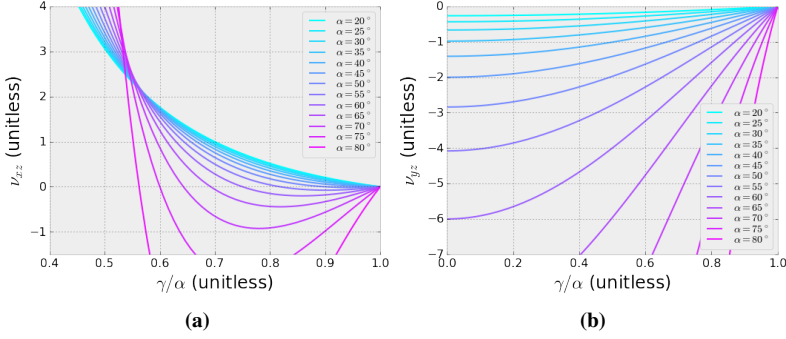$$\frac{dx}{d\gamma} = 4s\cos 2\gamma \tag{6}$$

(a)

(b)

Figure 5: *Poisson ratios of Tachi-Miura honeycomb. A) $\nu_{xz} = -\varepsilon_x/\varepsilon_z$, B) $\nu_{yz} = -\varepsilon_y/\varepsilon_z$.*

$$\frac{dy}{d\gamma} = -2s\sin 2\gamma \tag{7}$$

$$\frac{dz}{d\gamma} = \frac{dz}{d\beta}\frac{d\beta}{d\gamma} = Nd\cos\beta\frac{d\beta}{d\gamma} = Nd\frac{-1}{\tan\beta\tan\alpha\cos^2\gamma} \tag{8}$$

where the final line follows from implicitly differentiating the governing equation. Now we calculate the strains:

$$\varepsilon_x = \frac{dx}{x} = \frac{dx}{d\gamma}\frac{d\gamma}{x} = \frac{d\gamma(1-\tan^2\gamma)}{\tan\gamma} \tag{9}$$

$$\varepsilon_y = \frac{dy}{y} = \frac{dy}{d\gamma}\frac{d\gamma}{y} = -2d\gamma\tan\gamma \tag{10}$$

$$\varepsilon_z = \frac{dz}{z} = \frac{dz}{d\gamma}\frac{d\gamma}{z} = \frac{-d\gamma\tan\gamma}{\tan^2\alpha\cos^2\gamma - \sin^2\gamma} \tag{11}$$

These expressions can be used directly to calculate the Poisson ratios, as the factor of $d\gamma$ cancels:

$$\nu_{xz} = -\frac{\varepsilon_x}{\varepsilon_z} \tag{12}$$

$$\nu_{yz} = -\frac{\varepsilon_y}{\varepsilon_z} \tag{13}$$

These values are shown in Figure 5. We see that the Poisson ratio depends on the choice of α, but it is independent of d and N. Further, for many choices of α and over much of the folding range, ν_{xz} is approximately zero, while ν_{yz} is very sensitive to α over this same range. Thus, by selecting α, we can control the Poisson properties of the honeycomb.
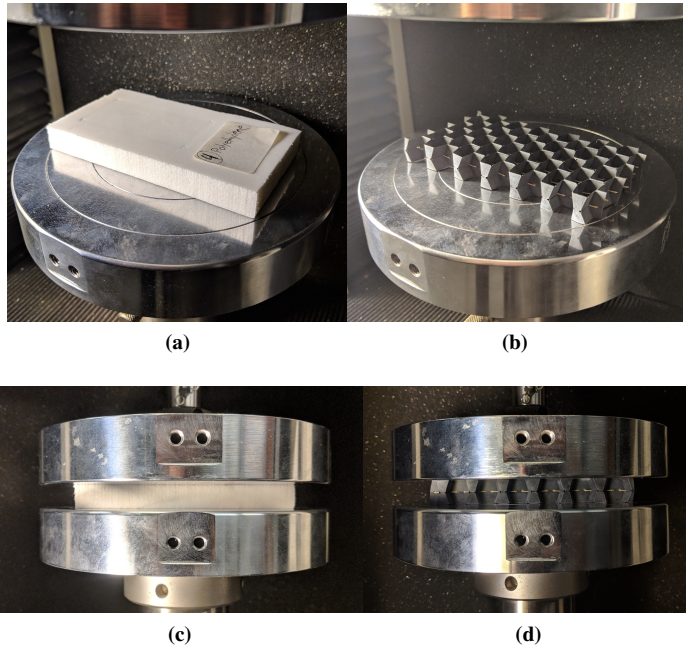
Figure 6: *A) Foam sample on test platen, B) Folded sample on test platen, C) Foam sample loaded by platens, D) Folded sample loaded by platens.*

2.2 Elastic behavior testing

The behavior of Tachi-Miura honeycombs under realistic boundary conditions is a combination of the rigid mechanism analyzed above and elastic deformations of the underlying material. A nonzero Poisson ratio means that fixed or frictional boundary conditions effectively resist the structure's tendency to follow its rigid mechanism under a compressive load in the z direction [Yasuda et al. 13]. The larger the magnitude of the Poisson ratio, the more lateral movement is required by the rigid mechanism, and hence, the more resistance is offered from the boundary condition. As the average magnitude of the Poisson ratios v_{xz} and v_{yz} increases with α, we expect the effective stiffness of Tachi-Miura honeycombs subject to fixed or frictional boundary conditions to also increase with α.

To confirm this effect, we performed compression testing of Tachi-Miura honeycombs comparing the results to those of commercially available engineering foams. Using a constant base material and sheet thickness, we prepared samples with varying Miura angles. We stitched these samples to retain the folded state of the strip folds.

We applied a load of 100 N to the samples over their full area of 54 cm^2, cycling the load six times at a rate of 1 mm per minute. We tested commercial foam samples of several materials having similar density to the pleated honeycomb samples with
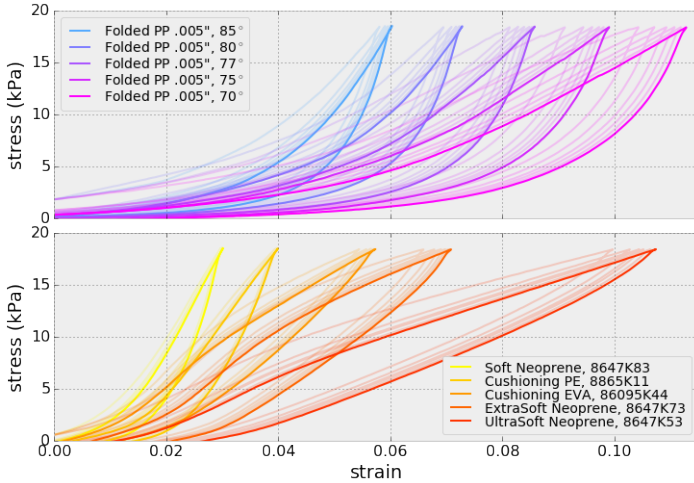
Figure 7: *Loading curves of Tachi-Miura polyhedra compared with those of engineering foams*

the same test parameters. The results (graphed in Figure 7) show the the pleated honeycombs span a range of average modulus from roughly 140 to 300 kPa, while the commercial foams range from roughly 170 to 500 kPa.

This shows that by using a single material and simply changing the Miura angle, we can produce a similar range of stiffness as is exhibited by a range of commercial foams. The conventional foams use a variety of materials and process parameters to achieve this range of stiffness. Thus, the reduction of material properties to geometry has the potential to simplify the manufacturing supply chains for products using foam-like materials. Further, foams are commonly made in a heat-induced expansion process, giving no ability to spatially vary material properties. Tachi-Miura honeycombs can be constructed where Miura angle varies from cell to cell, effectively giving the ability to spatially map stiffness. While polyhedra with differing Miura angle are not strictly tileable, similar methods as outlined above can work in practice to produce such honeycombs with only minor gaps between adjacent cells. Quantifying the precise limits to this approach is an active area of future research.

2.3 Shoe sole prototype

Given that Tachi-Miura honeycombs can exhibit similar compliance as commercial foams while filling a prescribed shape, we now use our construction to prototype a running shoe sole. The thermal processes involved in creating a conventional sole are responsible for nearly half of the energy required to manufacture an athletic shoe [Cheah et al. 13], and so creating a sole using only cutting and folding processes is an attractive strategy for embodied energy reduction. Further, athletic

soles are conventionally produced in a machined mold, requiring a large number of identical soles to be produced for economic feasibility. Specifying the sole geometry using the fold pattern instead of a mold has the potential to enable customized shoes without this overhead.

Figure 8 shows the steps of producing this folded running shoe sole. First, the geometry is digitally designed. In this case, the sole has a thickness of 20mm throughout the heel and tapers to 10mm through the forefoot. The footprint of cells which are populated with Tachi-Miura polyhedra are selected to fit inside the shape of common mens size 10 sole outline. The angle α is 50°, while the lengths d and s are 2.8mm and 8.8mm, respectively. The top three images at left of Figure 8 show the three-dimensional design and the corresponding folding and cutting pattern.
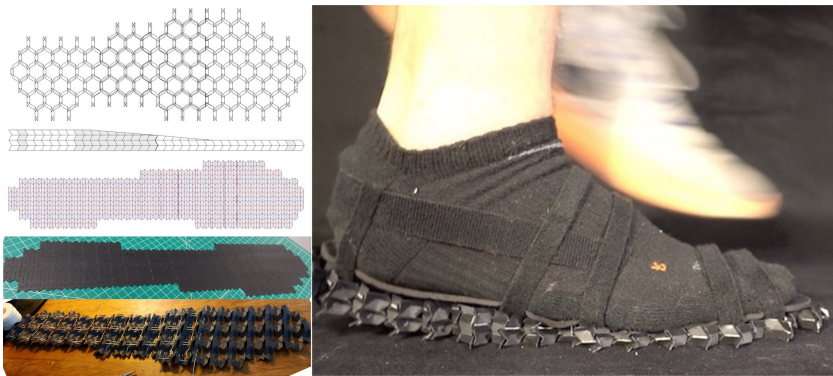

Figure 8: *A) Plan view of digitally designed geometry for shoe sole, B) Altitude view, C) Cut and fold pattern for shoe sole, D) Laser cut polypropylene prototype, E) After initial folding, F) Testing the shoe sole at running speed.*

This pattern is sent to a laser-cutter, where the outline and slits are through-cut and the creases are half-cut. The material used is 0.25mm polypropylene, which produces robust creases with this laser processing technique. This sheet is then folded with the aid of 3D printed creasing dies of progressively larger fold angles γ. The flat and folded states are shown in the bottom two images at the left of Figure 8, and the folding motion is shown in this video. Finally, cotton thread is passed through laser cut holes and pulled tight in order to keep the strip folds held closed. The finished shoe is shown in Figure 8 at right during a running test.

When loaded by a footstep, the folded shoe sole compresses to levels similar to that of a conventional foam shoe, absorbing the impact of the foot strike. At this point, the forces arising from the Poisson effects and boundary conditions balances the force from the foot, and the Tachi-Miura honeycomb is limited from continuing its flat-folding mechanism. The deformation occurs chiefly at regions of highest force (for example, under the heel and metatarsal heads), effectively conforming to the underfoot shape. With a thin neoprene sock liner, the result was comfortable for a range of test athletes. This video shows high speed video of the shoe sole in

use at running speeds.

3 Conclusions

We have shown how existing techniques for producing shaped hexagonal-celled honeycombs can be adapted to produce shaped honeycombs with Tachi-Miura polyhedra as cells. The bi-directional flat folding mechanism of the Tachi-Miura polyhedron endows the resulting honeycombs with the same flat foldings. In physical prototypes, finite-thickness materials and boundary conditions turn this flat folding into an elastic mechanism, a powerful tool for building robust structures with compliance.

Motivated by this, we investigated the mechanical properties of Tachi-Miura honeycombs, first calculating the rigid Poisson ratios. Next, we compared the mechanical behavior of the structures to common engineering foams, showing it is possible to create a similar range of compliance by changing the angle α. Finally, we use these findings to design a prototype making use of both the compliance and the shape control: a running shoe sole.

In this work, we used 3D-printed creasing dies as a tool to fold the samples quickly. This was effective but required considerable manual labor. For future work, we will increase production rates by either automating the use of similar incremental forming dies, or using "pattern and gather" approaches [Schenk 12].

References

[Calisch and Gershenfeld 18] Sam Calisch and Neil Gershenfeld. "Towards continuous production of shaped honeycombs." In *ASME 2018 Manufacturing Science and Engineering Conference*. American Society of Mechanical Engineers, 2018.

[Cheah et al. 13] Lynette Cheah, Natalia Duque Ciceri, Elsa Olivetti, Seiko Matsumura, Dai Forterre, Richard Roth, and Randolph Kirchain. "Manufacturing-focused emissions reductions in footwear production." *Journal of Cleaner Production* 44 (2013), 18 – 29. Available online (http://www.sciencedirect.com/science/article/pii/S0959652612006300).

[Miura and Tachi 10] Koryo Miura and Tomohiro Tachi. "Synthesis of Rigid-Foldable Cylindrical Polyhedral." *Symmetry: Art and Science, International Society for the Interdisciplinary Study of Symmetry, Gmuend*. Available online (http://www.tsg.ne.jp/TT/cg/FoldableCylinders_miura_tachi_ISISSymmetry2010.pdf).

[Nojima and Saito 06] Taketoshi Nojima and Kazuya Saito. "Development of newly designed ultra-light core structures." *JSME International Journal Series A Solid Mechanics and Material Engineering* 49:1 (2006), 38–42. Available online (http://adsabs.harvard.edu/abs/2006JSMEA..49...38N).

[Saito et al. 11] Kazuya Saito, Fabio Agnese, and Fabrizio Scarpa. "A cellular kirigami morphing wingbox concept." *Journal of intelligent material systems and structures* 22:9 (2011), 935–944. Available online (http://jim.sagepub.com/content/22/9/935.refs).

[Saito et al. 14] Kazuya Saito, Sergio Pellegrino, and Taketoshi Nojima. "Manufacture of arbitrary cross-section composite honeycomb cores based on origami techniques." *Journal of Mechanical Design* 136:5 (2014), 051011. Available online (http://pressurevesseltech.asmedigitalcollection.asme.org/article.aspx?articleid=1831332).

[Schenk 12] Mark Schenk. "Folded shell structures." Ph.D. thesis, University of Cambridge, 2012. Available online (http://www.markschenk.com/research/files/PhD%20thesis%20-%20Mark%20Schenk.pdf).

[Tachi and Miura 12] Tomohiro Tachi and Koryo Miura. "Rigid-foldable cylinders and cells." *J. Int. Assoc. Shell Spat. Struct.* 53:4 (2012), 217–226. Available online (http://origami.c.u-tokyo.ac.jp/~tachi/cg/RigidFoldableCylindersCellsTachiMiuraJournalIASS2012.pdf).

[Wang et al. 17] Lijun Wang, Kazuya Saito, You Gotou, and Yoji Okabe. "Design and fabrication of aluminum honeycomb structures based on origami technology." *Journal of Sandwich Structures & Materials* 0:0 (2017), 1099636217714646. doi:10.1177/1099636217714646. Available online (https://doi.org/10.1177/1099636217714646).

[Yasuda and Yang 15] H Yasuda and Jinkyu Yang. "Reentrant Origami-Based Metamaterials with Negative Poisson's Ratio and Bistability." *Physical review letters* 114:18 (2015), 185502. Available online (http://faculty.washington.edu/jkyang/research/publication/2015_PRL_origami.pdf).

[Yasuda et al. 13] Hiromi Yasuda, Thu Yein, Tomohiro Tachi, Koryo Miura, and Minoru Taya. "Folding behaviour of Tachi–Miura polyhedron bellows." In *Proc. R. Soc. A*, 469, 469, p. 20130351. The Royal Society, 2013. Available online (http://rspa.royalsocietypublishing.org/content/469/2159/20130351.short).

[Yasuda et al. 16] H. Yasuda, C. Chong, E. G. Charalampidis, P. G. Kevrekidis, and J. Yang. "Formation of rarefaction waves in origami-based metamaterials." *Phys. Rev. E* 93 (2016), 043004. doi:10.1103/PhysRevE.93.043004. Available online (https://link.aps.org/doi/10.1103/PhysRevE.93.043004).

Sam Calisch
Center for Bits and Atoms, Massachusetts Institute of Technology, Cambridge, MA, U.S.A.
e-mail: sam.calisch@cba.mit.edu

Neil Gershenfeld
Center for Bits and Atoms, Massachusetts Institute of Technology, Cambridge, MA, U.S.A.
e-mail: neil.gershenfeld@cba.mit.edu

Acknowledgement